Data Mining and Machine Learning on the Basis from Reflexive Eye Movements Can Predict Symptom Development in Individual Parkinson's Patients

Andrzej W. Przybyszewski[1,2], Mark Kon[3], Stanislaw Szlufik[4], Justyna Dutkiewicz[4], Piotr Habela[2], and Dariusz M. Koziorowski[4]

[1]University of Massachusetts Medical School, Dept Neurology, Worcester, MA 01655, USA, Andrzej.Przybyszewski@umassmed.edu
[2]Polish-Japanese Institute of Information Technology, 02-008 Warszawa, Poland {przy,piotr.habela@pjwstk.pl
[3]Mathematics and Statistics, Boston University, Boston, MA 02215, USA mkon@bu.edu
[4]Neurology, Faculty of Health Science, Medical University Warsaw, Poland stanislaw.szlufik@gmail.com, justyna_dutkiewicz@wp.pl, dkoziorowski@esculap.pl

Abstract. We are still not in a position to understand most of the brain's deeper computational properties. As a consequence, we also do not know how brain processes are affected by nerve cell deaths in neurodegenerative diseases (ND). We can register symptoms of ND such as motor and/or mental disorders (dementias) and even provide symptomatic relief, though the structural effects of these are in most cases not yet understood. Fortunately, with early diagnosis there are often many years of disease progression with symptoms that, when they are precisely monitored, may result in improved therapies. In the case of Parkinson's disease, measurements of eye movements can be diagnostic. In order to better understand their relationship to the underlying disease process, we have performed measurements of reflexive eye movements in Parkinson's disease (PD) patients. We have compared our measurements and algorithmic diagnoses with experts' diagnoses. The purpose of our work was to find universal rules, using rough set theory, to classify how condition attributes predict the neurologist's diagnosis. Prediction of individual UPDRS values only from reflexive saccade (RS) latencies was not possible. But for n = 10 patients, the patient's age, latency, amplitude, and duration of RS gave a global accuracy in individual patients' UPRDS predictions of about 80%, based on cross-validation. This demonstrates that broadening the spectrum of physical measurements and applying data mining and machine learning (ML) can lead to a powerful biomarker for symptom progression in Parkinson's.

Keywords: Neurodegenerative disease, rough set, decision rules.

1 Introduction

The majority of neurologists use their experience based largely on statistical intuition to analyze symptom development in Parkinson's disease (PD) patients. By applying

A. Gelbukh et al. (Eds.): MICAI 2014, Part II, LNAI 8857, pp. 499–509, 2014.

statistics based on analysis of large databases one can find significant information about the specificity of PD. But, due to a variety of cares, some results obtained even from the most prominent experts might be inconsistent. Applying standard, statistical averaging methods to such inconsistent information may give confusing results even leading to conclusions that a specific care does not effectively work in "averaged" PD patient. We might face similar challenges when studying factors that might lead to longer, better, and more active lives for people with Parkinson's. Various neurologists may also interpret differently the meanings of the UPDRS that result different therapies. These problems are articulated in the popular statement "No two people face Parkinson's in quite the same way." People vary substantially in their combination of symptoms, rate of progression, and reaction to treatment. As mentioned, averaging patients' symptoms to measure effects of different therapies can give very crude approximation of actual outcomes. If we want to improve such analyses, we must take into account the great variety of patients' symptoms and inconsistent effects of care in different PD cases.

For this reason, we propose to extend statistical analysis of PD outcomes using data mining and machine learning (ML) methods that give a more standardized interpretation of individual patient's symptoms and development. As a consequence it is possible that these methods may suggest specific treatments adjusted to different individual patients that may lead to slowing of symptoms and improvements in quality of life. Such analysis is proposed on the basis of learning algorithms that intelligently process data of individual patients in a standardized and specific ways. Our symptom classification method strives to emulate other means of complex object recognition such as those in visual systems. The ability of natural vision to recognize objects arises in the afferent, ascending pathways that classify properties of objects' parts from simple attributes in lower sensory areas, to more complex ones, in higher analytic areas. The resulting classifications are compared and adjust by interaction with whole object ("holistic") properties (representing the visual knowledge) at all levels using interaction with descending pathways [1] that was confirmed in animal experiments [2]. These interactions at multiple levels between measurements and prior knowledge can help to differentiate individual patient's symptoms and response treatments variability in a way similar to a new, complex object inspection [3, 4]. Machine learning algorithms for analyzing subtle signal variations will hopefully lead to better analysis of individual patients' conditions.

Diagnostic findings of neurologists are based on interaction of their measurements and experience. In the most cases, they estimate values of the Hoehn and Yahr scale and the UPDRS (Unified Parkinson's Disease Rating Scale). However, these are not always precise and can be partially subjective. In our data mining approach we use the neurologist's diagnosis as decision attributes and measurements as condition attributes.

2 Methods

Our experiments were performed on ten Parkinson Disease (PD) patients who had undergone the Deep Brain Stimulation (DBS) surgery mainly for treatment of their motor symptoms. They were qualified for the surgery and observed postoperatively in the Dept. of Neurology and got surgical DBS implementation in the Institute of

Neurology and Psychiatry WUM [5]. We conducted horizontal RS (reflexive saccades) measurements in ten PD patients during four sessions designed as S1: MedOffDBSOff, S2: MedOffDBSOn, S3: MedOnDBSOff, S4: MedOnDBSOn. During the first session (S1) the patient was off medications (L-Dopa) and DBS stimulators was OFF; in the second session (S2) the patient was off medication, but the stimulator was ON; in the third session (S3) the patient was after his/her doses of L-Dopa and the stimulator was OFF, and in the fourth session (S4) the patient was on medication with the stimulator ON. Changes in motor performance, behavioral dysfunction, cognitive impairment and functional disability were evaluated in each session according to the UPDRS. The reflexive saccades (RS) were recorded by head-mounted saccadometer (Ober Consulting, Poland). We have used an infrared eye track system coupled with a head tracking system (JAZZ-pursuit – Ober Consulting, Poland) in order to obtain high accuracy and precision in eye tracking and to compensate possible subjects' head movements relative to the monitor. Thus subjects did not need to be positioned in an unnatural chinrest.

A patient was sited at the distance of 60-70 cm from the monitor with head supported by a headrest in order to minimize head motion. We measured fast eye movements in response to a light spot switched on and off, which moved horizontally from the straight eye fixation position (0 deg) to 10 deg to the left or 10 deg to the right after arbitrary time ranging between 0.5–1.5 s. When the patient fixated eyes on the spot in the middle marker (0 deg) the spot then changed color from white to green, indicating a signal for performance of RS (reflexive saccades); or from white to red meaning a signal for performing AS (antisaccades). Then the central spot was switched off and one of the two peripheral targets, selected at random with equal probability, was illuminated instead. Patients had to look at the targets and follow them as they moved in the RS task or made opposite direction saccades in the AS task. After making a saccade to the peripheral target, the target remained on for 0.1 s after which another trial was initiated.

In each test the subject had to perform 20 RS and 20 AS in a row in Med-off (medication off) within two situations: with DBS off (S1) and DBS on (S2). In the next step the patient took medication and had a break for one half to one hour, and then the same experiments were performed, with DBS off (S3) and DBS on (S4). In this work we have analyzed only RS data using the following population parameters averaged for both eyes: delay mean (+/-SD –standard deviation); amplitude mean (+/-SD); max velocity mean (+/-SD); duration mean (+/-SD).

2.1 Theoretical Basis

The structure of data is an important point of our analysis. Here we represent it in the form of information system or a decision table. We define such an information system (after Pawlak [6]) as a pair $S = (U, A)$, where U, A are nonempty finite sets called the *universe of objects* and the *set of attributes*, respectively. If $a \in A$ *and* $u \in U$, the value $a(u)$ is a unique element of V (where V is a value set).

The *indiscernibility relation* of any subset B of A or $IND(B)$, is defined [6] as follows: $(x, y) \in IND(B)$ or $xI(B)y$ if and only if $a(x) = a(y)$ for every $a \in B$, where $a(x) \in V$. $IND(B)$ is an equivalence relation, and $[u]_B$ is the equivalence class of u, or a *B-elementary granule*. The family of all equivalence classes of $IND(B)$ will be denoted $U/I(B)$ or U/B. The block of the partition U/B containing u will be denoted by $B(u)$.

We define a **lower approximation** of symptoms set $X \subseteq U$ in relation to a symptom attribute B as $\underline{B}X = \{u \in U: [u]_B \subseteq X\}$, and the **upper approximation** of X as $\overline{B}X = \{u \in U: [u]_B \cap X \neq \phi\}$. In other words, all symptoms are classified into two categories (sets). The lower movement approximation set X has the property that all symptoms with certain attributes are part of X, and the upper movement approximation set has property that only some symptoms with attributes in B are part of X (for more details see [5]). The difference of $\overline{B}X$ *and* $\underline{B}X$ is defined as the boundary region of X i.e., $BN_B(X)$. If $BN_B(X)$ is empty set than X is *exact* (*crisp*) with respect to B; otherwise if $BN_B(X) \neq \phi$ and X is not *exact* (i.e., it is *rough*) with respect to B. We say that the B-lower approximation of a given set X is union of all *B-granules* that are included in X, and the B-upper approximation of X is of the union of all *B-granules* that have nonempty intersection with X.

The system S will be called a decision table $S = (U, C, D)$ where ***C* is the condition** and ***D* is the decision attribute** [6]. In the table below (Table 2), as an example, the decision attribute D, based on the expert opinion, is placed in the last column, and condition attributes measured by the neurologist, are placed in other columns. **On the basis of each row in the table, rules describing the condition of each patient can be proposed.** As the number of rules is same as the number of rows, these rules can have many particular conditions. The main concept of our approach is to describe different symptoms in different patients by using such rules. On the basis of such rules, using the **modus ponens principle** we wish to find universal rules to relate symptoms and treatments in different patients.

However, symptoms even for the same treatments are not always the same; therefore **our rules must have certain "flexibility", or granularity, which can be interpreted as the probability of finding certain symptoms in a group of patients under consideration. The granular computation simulates the way in which neurologists interact with patients.** This way of thinking relies on the ability to perceive a patient's symptoms under various levels of granularity (i.e., abstraction) in order to abstract and consider only those symptoms that serve to determine a specific treatment and thus to switch among different granularities. By focusing on different levels of granularity, one can obtain different levels of knowledge, as well as a greater understanding of the inherent knowledge structure. Granular computing is thus essential in human intelligent problem solving behaviors in *problem-specific* tasks.

We define the notion of a reduct $B \subset A$. The set B is a reduct of the information system if $IND(B) = IND(A)$ and no proper subset of B has this property. In case of decision tables decision reduct is a set $B \subset A$ of attributes which cannot be further reduced and $IND(B) \subset IND(d)$. A decision rule is a formula of the form $(a_{i1} = v_1) \wedge ... \wedge (a_{ik} = v_k) \Rightarrow d = v_d$, where $1 \leq i_1 < ... < i_k \leq m$, $v_i \in Va_i$. Atomic subformulas $(a_{i1} = v_1)$ are called conditions. We say that rule r is applicable to object, or alternatively, the object

matches rule, if its attribute values satisfy the rule. With a rule we can connect some numerical characteristics such as matching and support. We can replace the original attribute a_i with new, binary attributes which indicate whether actual attribute value for an object is greater or lower than c (see [7]), we define c as a cut. Thus a cut for an attribute $a_i \in A$, with V_{ai} will be a value $c \in V_{ai}$. A template of A is a propositional formula $v_i \in V_{ai}$. A generalized template is a formula of the form $\wedge(a_i \in T_i)$ where $T_i \subset V_{ai}$. An object satisfies (matches) a template if for every attribute a_i we have $a_i = v_i$ where $a_i \in$ A. The template is a natural way to split the original information system into two distinct sub-tables. One of these sub-tables consists of the objects that satisfy the template, while the second contains all others. A *decomposition tree* is defined as a binary tree, whose every internal node is labeled by some template and external node (leaf) is associated with a set of objects matching all templates in a path from the root to a given leaf [8].

In a second test we have divided our data into two or more subsets. By training on all but one of these subsets (the training set) using machine learning (ML), we obtained classifiers that when applied to the remaining (test) set gave new numerical decision attributes, well correlated with neurologist decision attributes (based on a confusion matrix).

3 Results

The patients' mean age was 51.1±10.2(SD) years, mean disease duration was 11.3±3.2 years, mean UPDRS (related to all symptoms): S1: 66.6±13.8 S2: 30.0±16.3; S3: 58.1±13.5; S4: 22.3±13.6; mean UPDRS III (related only to motor symptoms): S1: 42.7±11.3 S2: 17.8±10.6; S3: 34.1±10.8; S4: 10.9±8.3; mean RS latencies: S1:291.2±93.1ms, S2: 199.6±39.5ms, S3: 232.9±82.7ms; S4: 183.2±30ms.

Differences between latencies: S1-S2, and S1-S4 were statistically significant (t-test $p< 0.01$) even when they were variable in individual patients (Fig. 1), while S1-S3 was not statistically significant, this is similar to differences between UPDRS/UPDRS III: S1-S2, and S1-S4 were statistically significant ($t< 0.001$) and S1-S3 was not statistically significant.

Other parameters of RS did not change significantly with the session number.

3.1 Rough Set and Machine Learning Approach

As described above we have used the RSES 2.2 (Rough System Exploration Program) [8] in order to find regularities in our data. At first our data was placed in the information table as originally proposed by Pawlak [6].

The full table has 15 attributes and 36 objects (measurements). In the Table 1 are values of 11 attributes for two patient: P# - patient number, age – patient's age, sex – patient's sex: 0 - female, 1 – male, t_dur – duration of the disease, S# - Session number, UPDRS – total UPDRS, HYsc – Hoehn and Yahr scale all measured by the neurologist and saccades measurements: SccDur - saccade duration; SccLat - saccade latency; SccAmp – saccade amplitude, and SccVel – saccade velocity.

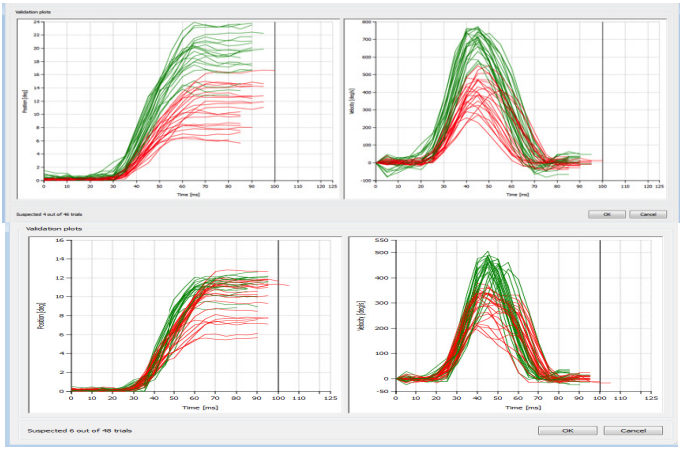

Fig. 1. An example of experimental recordings from Pat #38 in two sessions: upper plots from session S1: MedOFF & StimOFF; lower plots from session S4: MedON & StimON; left plots show latency measurements, right plots – saccades' amplitude and velocity. Notice change in variability of responses between S1 and S4.

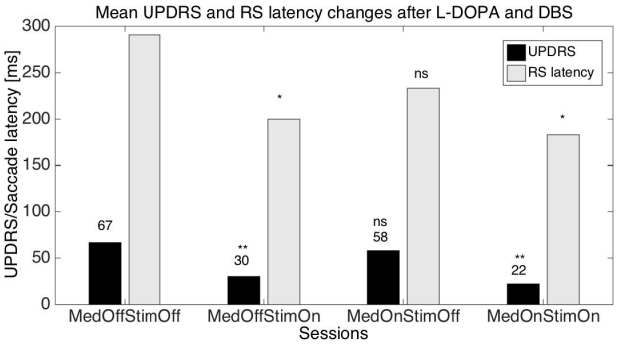

Fig. 2. This graph shows parallel changes in UPDRS and reflexive saccade latencies as effects of medication and stimulation. Changes between control and MedOnStimOn were significantly different for UPDRS $p<0.001$ (**), RS $p<0.01$ (*).

Table 1. Extract from the information table

P#	age	sex	t_dur	S#	UPDRS	HYsc	SccDur	SccLat	SccAmp	SccVel
28	54	1	8	1	58	2.0	43	402	12	566,9
28	54	1	8	2	40	1.0	46	297	11	474,5
28	54	1	8	2	40	1.0	49	227	10	431,2
28	54	1	8	4	16	1.0	47	198	9	376,2
38	56	0	11	1	49	2.5	42	285	14	675,2
38	56	0	11	2	22	1.5	48	217	12	509,7
38	56	0	11	3	37	2.5	43	380	14	638,9
38	56	0	11	4	12	1.5	45	187	10	482,6

In the next step, we have performed reduction of attributes (see reduct in the Method section) to a minimum number of attributes describing our results. We have also created a discretization table: here single values of measurements were replaced by their range (as describe in the Method section on cut sets). As the result we have obtained the decision table (Table 2 –see below).

Table 2. Part of the decision discretized-table

Pat#	age	t_dur	S#	HYsc	SccDur	SccLat	SccAmp	UPDRS
'28	"(-Inf,55.0)"	*	1	*	"(-Inf,45.5)"	"(260.0,Inf)"	"(10.5,Inf)"	"(55.0,Inf)"
'28	"(-Inf,55.0)"	*	2	*	"(45.5,Inf)"	"(260.0,Inf)"	"(10.5,Inf)"	"(22.5,55.0)"
28	"(-Inf,55.0)"	*	2	*	"(45.5,Inf)"	"(-Inf,260.0)"	"(-Inf,10.5)"	"(22.5,55.0)"
:28	"(-Inf,55.0)"	*	4	*	"(45.5,Inf)"	"(-Inf,260.0)"	"(-Inf,10.5)"	"(14.0,22.5)"
'38	"(55.0,Inf)"	*	1	*	"(-Inf,45.5)"	"(260.0,Inf)"	"(10.5,Inf)"	"(22.5,55.0)"
'38	"(55.0,Inf)"	*	2	*	"(45.5,Inf)"	"(-Inf,260.0)"	"(10.5,Inf)"	"(14.0,22.5)"
'38	"(55.0,Inf)"	*	3	*	"(-Inf,45.5)"	"(260.0,Inf)"	"(10.5,Inf)"	"(22.5,55.0)"
'38	"(55.0,Inf)"	*	4	*	"(-Inf,45.5)"	"(-Inf,260.0)"	"(-Inf,10.5)"	"(-Inf,14.0)"

In the first column is the patient's number, in the second the patient's age divided in our group into patients below (Pat#28) or above (Pat#38) 55 years of age; disease duration and Hoehn and Yahr scale were not considered important (stars), along with session number; and other parameters of saccades were also divided into ranges. It is interesting to note how the UPDRS were divided into different ranges: above 55, 22.5 to 55, 14 to 22.5, and below 14 (the last column). On the basis of this decision table we can write the following rule:

('Pat'=28)&('age'="(-Inf,55.0)")&('Sess'=1)&('SccDur'="(-Inf,45.5)")&('SccLat' ="(260.0,Inf)")& (' SccAmp')="(10.5,Inf)") => ('UPDRS'="(55.0,Inf)") (1)

We read this formula above (eq. 1), as stating that each row of the table (Table 1) can be written in form of this equation (eq. 1). It states that if we evaluate patient #28 *and* with age below 55 *and* in session #1 *and* with saccade duration below 45.5 *and* saccade latency above 260 *and* … *and* saccade amplitude above 10.5 *then* patient's UPDRS is above 55.

These equations are parts of a data mining system bases on rough set theory [6]. We have tested our rule using the machine-learning concept. Randomly dividing our data into 6 groups, we took 5 groups as training set and tested the fourth. By changing groups belonging to the training and test sets, we have removed the effect of accidental group divisions. The results of each test were averaged – thus we have performed a 6-fold cross-validation. The results are gives as a confusion matrix (Table 3). As a machine-learning algorithm we have used the decomposition tree (see Methods).

We have performed several tests trying to predict UPDRS values on the basis of measures saccades properties. As changes in UPDRS and saccade latencies were similar when the session number was changed (Fig.2) we tried to predict individual UPDRS values only from RS latencies. Here however, we did not get good results. When to the session number, patient age, RS: latency, amplitude, and duration were added, the global accuracy in UPRDS prediction was about 80% (ML: decomposition

tree, cross-validation-method). This is good result for such a small population showing power of the data mining and machine learning methods in this type of neurological analysis. As UPDRS is a standard measurement in PD, the above results give the possibility of at least partly replace or augmenting neurologist estimates with the eye movements (EM) measurement results.

Table 3. Confusion matrix for different session numbers (S1-S4)

		Predicted				
		55.0, Inf	**22.5, 55.0**	**-Inf, 14.0**	**14.0, 22.5**	**ACC**
Actual	**55.0, Inf**	0.3	0.3	0	0	**0.2**
	22.5, 55.0	0	1.5	0	0	**1**
	-Inf, 14.0	0.0	0.3	0	0.2	**0**
	14.0, 22.5	0	0	0	0	**0**
	TPR	**0.2**	**0.8**	**0**	**0**	

TPR: True positive rates for decision classes, ACC: Accuracy for decision classes: the global coverage was 0.44, the **global accuracy was 0.79**, coverage for decision classes: 0.2, 0.5, 0.3, 0.0.

Another question that result is, whether EM can help to estimate possible effects of different treatments in individual patients? In order to demonstrate an answer, we have removed EM measurements and added other typically measured attributes such as: the Schwab and England ADL Scale, and UPDRS III and UPDRS IV to the decision table and tried to predict the effects of different treatments as represented by sessions 1 to 4 (medication and stimulation effects). Table 4 is a part of full decision discretized-table with decision attributes – the session number placed in the last column. On the basis of this table we have formulated rules using a rough set system and tested them with randomly divided data into 6 groups. We took 5 as training set (using ML protocol) and tested with sixth. In order to remove effect of the accidental division we have exchanged training and test groups and averaged results placed in the confusion matrix (Tabel 5).

Table 4. Part of the decision discretized-table **without** eye movement measurements

Pat#	age	t_dur	SEngs	UPDRS III	UPDRS IV	UPDRS	Sess#
"(27.5,41.5)"	"(43.5,Inf)"	*	"(-Inf, 75)"	"(36.0,46.0)"	"(10.5,Inf)"	"(1.75,Inf)"	1
"(27.5,41.5)"	"(43.5,Inf)"	*	"(75, Inf)"	"(13.0,26.0)"	"(10.5,Inf)"	"(-Inf,1.75)"	2
"(27.5,41.5)"	"(43.5,Inf)"	*	"(75, Inf)"	"(-Inf,6.0)"	"(10.5,Inf)"	"(-Inf,1.75)"	4
"(27.5,41.5)"	"(43.5,Inf)"	*	"(-Inf, 75)"	"(26.0,36.0)"	"(10.5,Inf)"	"(1.75,Inf)"	1
"(27.5,41.5)"	"(43.5,Inf)"	*	"(75, Inf)"	"(13.0,26.0)"	"(10.5,Inf)"	"(-Inf,1.75)"	2
"(27.5,41.5)"	"(43.5,Inf)"	*	"(-Inf, 75)"	"(13.0,26.0)"	"(10.5,Inf)"	"(1.75,Inf)"	3
"(27.5,41.5)"	"(43.5,Inf)"	*	"(75, Inf)"	"(-Inf,6.0)"	"(10.5,Inf)"	"(-Inf,1.75)"	4

Table 5. Confusion matrix for different session numbers (S1-S4)

		Predicted				
		1	**2**	**3**	**4**	**ACC**
Actual	**1**	0.5	0	0.5	0	**0.3**
	2	0	0.5	0	0.3	**0.4**
	3	0.8	0	0.2	0	**0.2**
	4	0	0.5	0	0.5	**0.4**
	TPR	**0.3**	**0.3**	**0.2**	**0.4**	

TPR: True positive rates for decision classes, ACC: Accuracy for decision classes: the global coverage was 0.64, the **global accuracy was 0.53**, coverage for decision classes: 0.5, 0.5, 0.75, 0.7.

We have performed the same procedures once more to test results of patients' eye movement influence on our predictions.

Table 6. Part of the decision discretized-table **with** eye movement measurements

Pat#	age	SccVel	UPDRS III	HYsc	SccDur	SccLat	SccAmp	Ses#
"(27.5,34.5)"*"(458.5,578.0)"	"(36, Inf)"	"(1.75,Inf)"	"(38,Inf)"	"(308.5,Inf)"	*			1
"(27.5,34.5)"*"(458.5,578)"	"(11.5,36)"	"(-Inf,1.75)"	"(38.0,Inf)"	"(-Inf,308.5)"	*			2
"(27.5,34.5)"*"(341.5,403)"	"(-Inf,11.5) "	"(-Inf,1.75)"	"(38,Inf)"	"(-Inf,308.5)"	*			4
"(34.5,Inf)" * "(665.5,Inf)"	"(11.5,36.0)"	"(1.75,Inf)"	"(38.0,Inf)"	"(-Inf,308.5)"	*			1
"(34.5,Inf)" * "(458.5,578)""	"(11.5,36)""	"(-Inf,1.75)"	"(38.0,Inf)"	"(-Inf,308.5)"	*			2
"(34.5,Inf)" * "(578.0,665.5)""	"(11.5,36)""	"(1.75,Inf)"	"(38.0,Inf)"	"(308.5,Inf)"	*			3
"(34.5,Inf)"*"(458.5,578)""	"(-Inf,11.1)"	"(-Inf,1.75)"	"(38, Inf)"	"(-Inf,308.5)"	*			4

Table 7. Confusion matrix for different session numbers (S1-S4)

		Predicted				
		1	**2**	**3**	**4**	**ACC**
Actual	**1**	0.8	0	0	0	**0.7**
	2	0	0.7	0	0	**0.7**
	3	0.2	0	0.8	0	**0.6**
	4	0	0.2	0	0.3	**0.25**
	TPR	**0.7**	**0.7**	**0.6**	**0.25**	

TPR: True positive rates for decision classes, ACC: Accuracy for decision classes, the global coverage was 0.5; the **global accuracy was 0.91**; coverage for decision classes: 0.6, 0.6, 0.6, 0.25.

As above, results of each test were averaged in a 6-fold cross-validation giving as the confusion matrix (Table 3). As a machine-learning algorithm we have used the decomposition tree (see Methods).

In summary, two last results have demonstrated that adding eye movement (EM) results to classical measurements performed by the most neurologists, can result in improved predictions of disease progression measured, as measured by improvement in global accuracy from 0.53 to 0.91. The EM measurements may also partly replaces neurological measurements such as the UPDRS, as global accuracy of the total UPDRS predictions taken from EM data was 0.79 for the above 10 PD patients.

4 Discussion

In current therapeutic protocols, even with the large numbers of approaches and clinical trials, there have still been few conclusive results on therapeutic identification and measurement of PD symptoms. There are multiple reasons for such failures: first, the shortcomings of current disease models in target validation and testing; second, difficulties in choosing clinical endpoints; third difficulties in finding sensitive biomarkers of disease progression. One clear problem is that the disease starts long before motor symptoms are observed, and another is that individual pathological mechanisms form a large spectrum. We have given an example comparing classical neurological diagnostic protocols with a new approach. The main difference between these types of measures is in their precision and objectivity. Our approach is doctor-independent and can be performed automatically. In the near future it may help in transforming some hospital-based to home-based treatments. In this scenario it will be possible to measure patient symptoms at home, and send these for consultation by neurologists. Such methods will be faster, more precise and can help with more frequent measurements. In consequence, they may help not only to determine more objectively a patient's symptoms, but also to follow up disease progression in more frequent intervals, something not possible currently, with the limited time resources of neurologists. If we obtain such information, it may lead to more appropriate therapies and the slowing down of disease progression. It is one of the purposes of this work to try to extract knowledge from symptoms in order further on to develop more appropriate therapies to stem disease progression.

5 Conclusions

We have presented a comparison of classical statistical averaging methods for PD diagnosis with rough set (RS) approaches. We used processed neurological data from PD patients in four different treatments and we have plotted averaged effects of the medication and brain stimulation in individual patients. As these effects are strongly patient dependent they could not give enough information to predict new patient's behavior. The RS and ML approaches are more universal giving general rules for predicting individual patient responses to treatments as demonstrated in UPDRS predictions.

Acknowledgements. This work was partly supported by projects Dec-2011/03/B/ST6/03816 and NN 518289240 from the Polish National Science Centre.

References

1. Przybyszewski, A.W.: The Neurophysiological Bases of Cognitive Computation Using Rough Set Theory. In: Peters, J.F., Skowron, A., Rybiński, H. (eds.) Transactions on Rough Sets IX. LNCS, vol. 5390, pp. 287–317. Springer, Heidelberg (2008)
2. Przybyszewski, A.W., Gaska, J.G., Foote, W., Pollen, D.A.: Striate cortex increases contrast gain of macaque LGN neurons. Visual Neuroscience 17, 1–10 (2000)
3. Przybyszewski, A.W.: Logic in Visual Brain: Compute to Recognize Similarities: Formalized Anatomical and Neurophysiological Bases of Cognition. Review of Psychology Frontier 1, 20–32 (2010) (open access)
4. Przybyszewski, A.W.: Logical rules of visual brain: From anatomy through neurophysiology to cognition. Cognitive Systems Research 11, 53–66 (2012)
5. Pizzolato, T., Mandat, T.: Deep Brain Stimulation for Movement Disorders. Frontiers in Integrative Neuroscience 6, 2 (2012), doi:10.3389/fnint.2012.00002
6. Pawlak, Z.: Rough sets: Theoretical aspects of reasoning about data. Kluwer, Dordrecht (1991)
7. Bazan, J., Son, N.H., Trung, T., Nguyen, S.A., Stepaniuk, J.: Desion rules synthesis for object classification. In: Orłowska, E. (ed.) Incomplete Information: Rough Set Analysis, pp. 23–57. Physica – Verlag, Heidelberg (1998)
8. Bazan, J., Szczuka, M.: RSES and RSESlib - A Collection of Tools for Rough Set Computations. In: Ziarko, W.P., Yao, Y. (eds.) RSCTC 2000. LNCS (LNAI), vol. 2005, pp. 106–113. Springer, Heidelberg (2001)